IEEE Access
Multidisciplinary | Rapid Review | Open Access Journal

Received February 10, 2022, accepted February 14, 2022, date of publication February 18, 2022, date of current version March 1, 2022.

Digital Object Identifier 10.1109/ACCESS.2022.3152802

Wideband Highly-Selective Bandpass Filtering Branch-Line Coupler

RUSAN KUMAR BARIK[1], (Member, IEEE), SLAWOMIR KOZIEL[1,2], (Fellow, IEEE), AND STANISLAW SZCZEPANSKI[2]

[1]Department of Engineering, Reykjavik University, 102 Reykjavík, Iceland
[2]Faculty of Electronics, Telecommunications and Informatics, Gdańsk University of Technology, 80-233 Gdańsk, Poland

Corresponding author: Slawomir Koziel (koziel@ru.is)

This work was supported in part by the Icelandic Centre for Research (RANNIS) under Grant 217771, and in part by the National Science Centre of Poland under Grant 2018/31/B/ST7/02369.

ABSTRACT This paper presents a novel design of a wideband highly-selective bandpass filtering branch-line coupler (FBLC). By integrating a coupled microstrip line, and an open-ended stub at each port of a single-section BLC, bandpass filtering characteristics with excellent selectivity and broad operating bandwidth have been achieved. The proposed circuit has been verified through EM simulations and physical measurements of the fabricated prototype. Experimental results demonstrate over 71-percent fractional bandwidth (2.25 GHz to 4.74 GHz) with a power imbalance lower than 0.5 dB. At the same time, the measured return loss and isolation are better than 15dB with the phase imbalance of $5 \pm 5°$. This level of performance, especially in terms of bandwidth and selectivity, has not been reported in the literature thus far.

INDEX TERMS Branch-line coupler, bandpass filtering, highly-selective, coupled-line.

I. INTRODUCTION

Branch-line couplers (BLCs) are indispensable components of numerous microwave systems. The 3-dB BLC delivers equal power split and 90-degree phase difference, which are the basic requirements for the realization of power amplifiers, balanced mixers, modulators, array antennas, filters, and matched attenuators. However, a conventional single-section BLC consists of quarter-wavelength transmission lines and exhibits narrow bandwidth, as well as unwanted harmonics. A number of techniques have been developed to achieve larger bandwidth, harmonic suppression, arbitrary power division, compact size, multi-band operation, and filtering response [1]–[21]. For example, bandwidth enhancement can be obtained by attaching impedance transformers to each port of the single-section BLC [1]–[3], utilization of two-section/three branch-line topologies [4]–[10], but also three-section/four branch-line topologies [11]–[18].

Suppression of unwanted harmonics, generated by, e.g., adjacent active components, is another consideration important in the design of modern wireless systems. The conventional 90-degree lines used for BLC design are unable to realize transmission zeros (TZs), which could be employed to suppress the harmonics. To implement the suppression, various equivalent circuits of 90-degree lines, such as L-shaped and open-ended stub [1], multiple π-shaped [3], open stub [7], unequal-length open stub [14, and coupled-line and open stub [16], [18], have been suggested. It should also be emphasized that wideband BLC topologies reported in [2], [4]–[6], [8]–[13], [15], [17], and [19], are not suitable to suppress the harmonics.

In recent years, several new topologies have been employed to realize wideband BLCs with improved performances in terms of bandwidth, compact size, and harmonic suppression [20]–[27]. In [20], the parallel coupled-lines have been attached to each port of the traditional single-section BLC to realize a wideband BLC with improved stopband response. The parallel coupled-line has been used extensively in the development of high-selectivity bandpass filter [21], filtering phase shifter [23], and matching condition for BLCs [24], [25] with improved bandwidth. The double-sided parallel strip-line has been employed to design a filtering 180° coupler in [22]. A branch-line coupler has been realized by using non-periodic stepped-impedance shunt stub in [26]. In [27], a flexible wideband three-section BLC has been designed by applying meandering technique on the paper substrate.

In RF front-end systems, the bandpass filters are integrated with another passive component to decrease the overall cost and size of the systems. In this context, the development

The associate editor coordinating the review of this manuscript and approving it for publication was Kai-Da Xu.

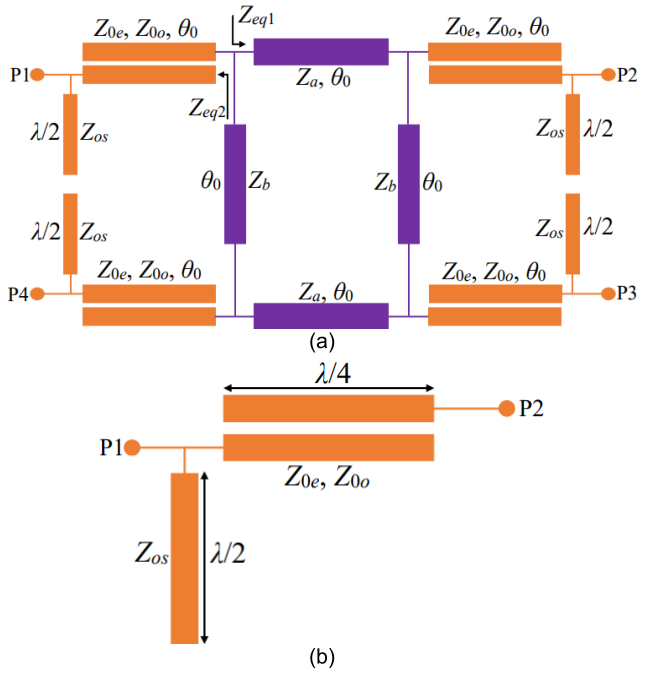

FIGURE 1. Proposed wideband FBLC: (a) design schematic, (b) additional transmission-line unit (ATLU).

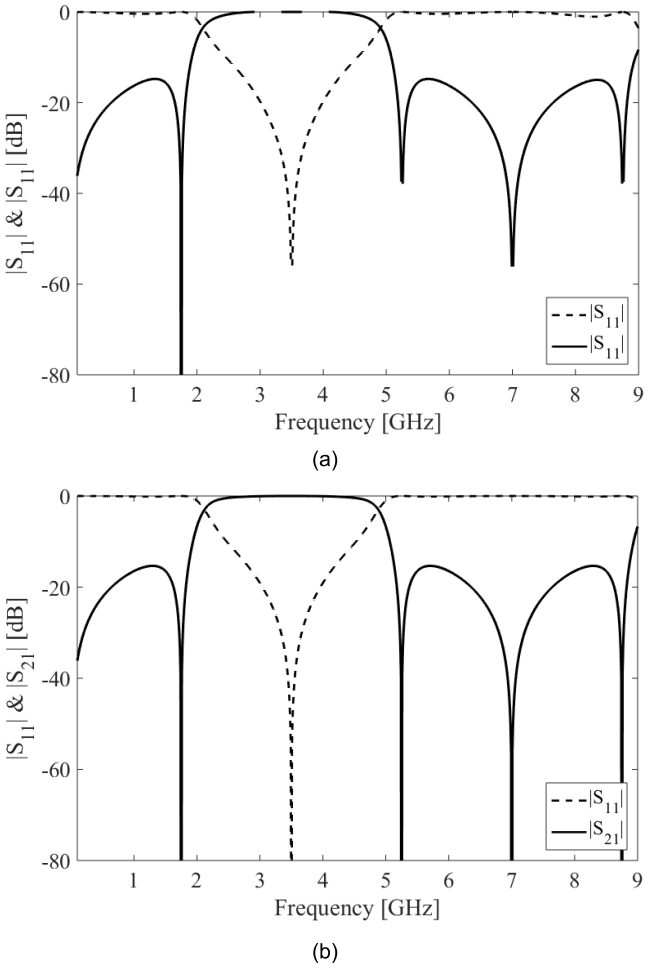

FIGURE 2. The S-parameters calculation: (a) analytical, (b) Keysight ADS circuit simulator.

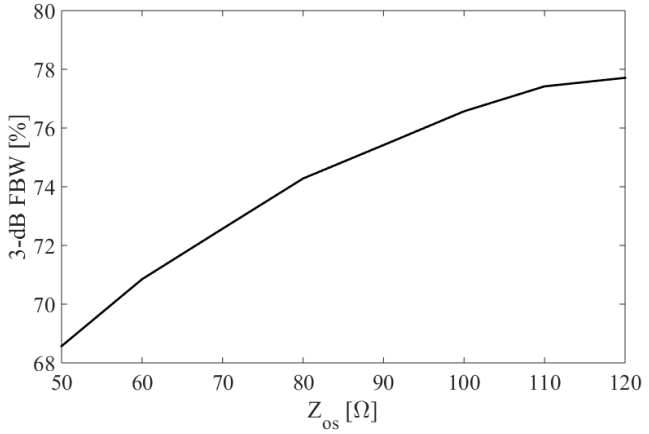

FIGURE 3. The variation of 3-dB FBW as a function of Z_{os}.

of filtering BLCs can be viewed as an attractive means of harmonic suppression, thereby paving the way to develop compact and cost-effective RF front-end systems [28]–[30]. A filtering BLC has been realized by using four half-wave resonators that generate one TZ in [28], but offers a narrow bandwidth of 61 MHz (2.47%). In [29], a filtering BLC has been designed by applying the source-load coupling that creates two TZs. This solution leads to diminishing the harmonics by 17 dB, yet the circuit bandwidth is only 3.17%. In [30], filtering K-inverters have been used as a replacement of conventional 90-degree lines to implement filtering BLC with wide stopband characteristics. This coupler achieves up to 5th harmonic suppression but features a narrow bandwidth. The applicability of the aforementioned filtering BLCs seems to be limited due to their extremely low bandwidth and selectivity. To further reduce the cost and the size of the RF front-end systems while ensuring broader bandwidth and high selectivity, novel coupler topologies should be developed and investigated.

In this work, a novel architecture of a filtering branch-line coupler (FBLC) with broad operating bandwidth and high selectivity has been designed, fabricated, and experimentally validated. In the proposed design, a coupled microstrip line and an open-ended stub are incorporated at each port of the single-section BLC to achieve filtering characteristics. The circuit produces four transmission zeros (TZs), which enable broadband harmonics elimination. Comprehensive benchmarking demonstrates the superiority of the presented BLC over state-of-the-art devices reported in the literature, especially in terms of wideband operation and selectivity.

II. DESIGN PROCEDURE

Figure 1(a) shows a schematic of the proposed wideband filtering BLC. Initially, a single-section BLC is constructed

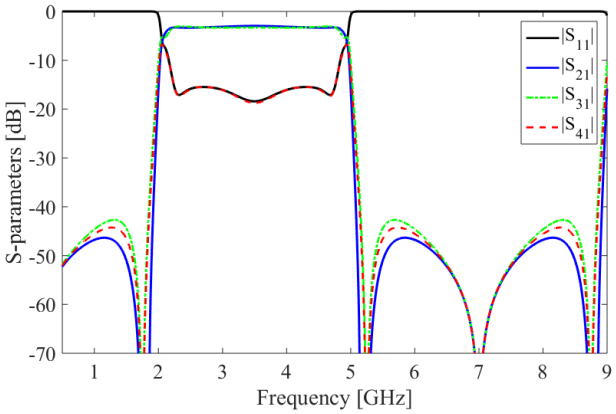

FIGURE 4. *S*-parameters of the proposed wideband highly-selective filtering BLC operating at 3.5 GHz.

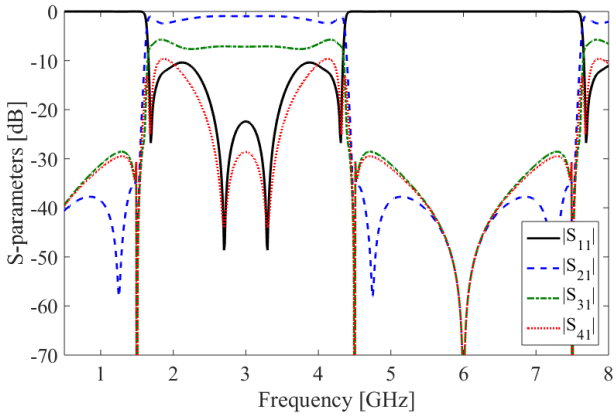

FIGURE 5. EM simulated magnitude responses of the proposed filtering coupler with *a* power division ratio of $k = 4$.

by using λ/4 lines (Z_a and Z_b) in a ring form, which is then modified by attaching an additional transmission-line unit (ATLU) at each port to achieve wideband filtering characteristic. Figure 1(b) shows the schematic of the proposed ATLU, which consists of a coupled-line (Z_{0e}, Z_{0o}, and λ/4), and an open-ended stub (Z_{os} and λ/4). The quarter-wavelength coupled-line provides a perfect matching condition to achieve wide bandwidth [31]. This bandwidth can be increased further by increasing the coupling. Hence, the coupling coefficient of the coupled line is obtained by carefully determining the even/odd-mode impedances. Also, the bandpass filtering responses are achieved due to the inherent properties of coupled lines. The bandpass rejection level and the selectivity of the filtering response increases by the use of the open-ended stub. The bandpass characteristic of the ATLU is investigated by analytical derivations.

The overall ABCD parameters of the ATLU are determined as the multiplication of individual transmission matrices of the open-ended stub and parallel coupled-line [32]:

$$\begin{bmatrix} A_T & B_T \\ C_T & D_T \end{bmatrix}_{ATLU} = \begin{bmatrix} A & B \\ C & D \end{bmatrix}_{OS} \begin{bmatrix} A & B \\ C & D \end{bmatrix}_{PCL} \tag{1}$$

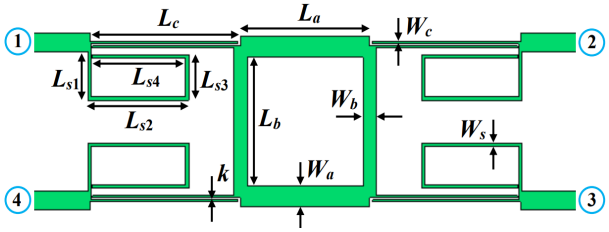

(a)

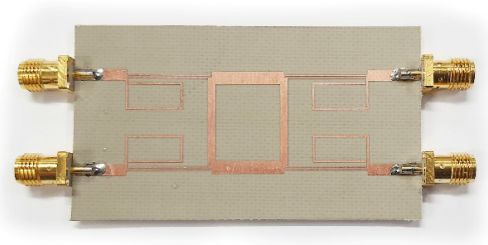

(b)

FIGURE 6. Proposed wideband FBLC: (a) final layout schematic; the optimized dimensions are $L_a = 16.68$, $W_a = 2.42$, $L_b = 17$, $W_b = 1.4$, $L_c = 15.64$, $W_c = 0.21$, $L_{s1} = 6.55$, $L_{s2} = 10.29$, $L_{s3} = 4.79$, $L_{s4} = 9.84$, $W_s = 0.369$. Units are in mm. (b) Photograph of the fabricated wideband FBLC.

Here,

$$\begin{bmatrix} A & B \\ C & D \end{bmatrix}_{PCL} = \begin{bmatrix} \frac{\rho_1}{\rho_2}\cos\theta_{oc} & j\frac{\rho_2^2 - \rho_1^2\cos^2\theta_{oc}}{2\rho_2\sin\theta_{oc}} \\ j\frac{2\sin\theta_{oc}}{\rho_2} & \frac{\rho_1}{\rho_2}\cos\theta_{oc} \end{bmatrix} \tag{2}$$

$$\begin{bmatrix} A & B \\ C & D \end{bmatrix}_{OS} = \begin{bmatrix} 1 & 0 \\ j\frac{\tan\theta_{os}}{Z_{os}} & 1 \end{bmatrix} \tag{3}$$

where, $\rho_1 = Z_{0e} + Z_{0o}$ and $\rho_2 = Z_{0e} - Z_{0o}$.

Equation (1) can be solved by substituting equations (2) and (3), which leads to the following expressions for each element of the matrix

$$A_T = \frac{\rho_1}{\rho_2}\cos\theta_{oc} \tag{4}$$

$$B_T = j\frac{\rho_2^2 - \rho_1^2\cos^2\theta_{oc}}{2\rho_2\sin\theta_{oc}} \tag{5}$$

$$C_T = j\frac{\rho_1}{Z_{os}\rho_2}\cos\theta_{oc}\tan\theta_{os} + j\frac{2\sin\theta_{oc}}{\rho_2} \tag{6}$$

$$D_T = \frac{\rho_1}{\rho_2}\cos\theta_{oc} - \frac{\rho_2^2 - \rho_1^2\cos^2\theta_{oc}}{2\rho_2\sin\theta_{oc}}\cdot\frac{\tan\theta_{os}}{Z_{os}} \tag{7}$$

The overall ABCD parameters are converted into Y-parameters using the following relationship [24]:

$$\begin{bmatrix} Y_{11} & Y_{12} \\ Y_{21} & Y_{22} \end{bmatrix} = \begin{bmatrix} \frac{D_T}{B_T} & -\frac{\Delta_T}{B_T} \\ -\frac{1}{B_T} & \frac{A_T}{B_T} \end{bmatrix} \tag{8}$$

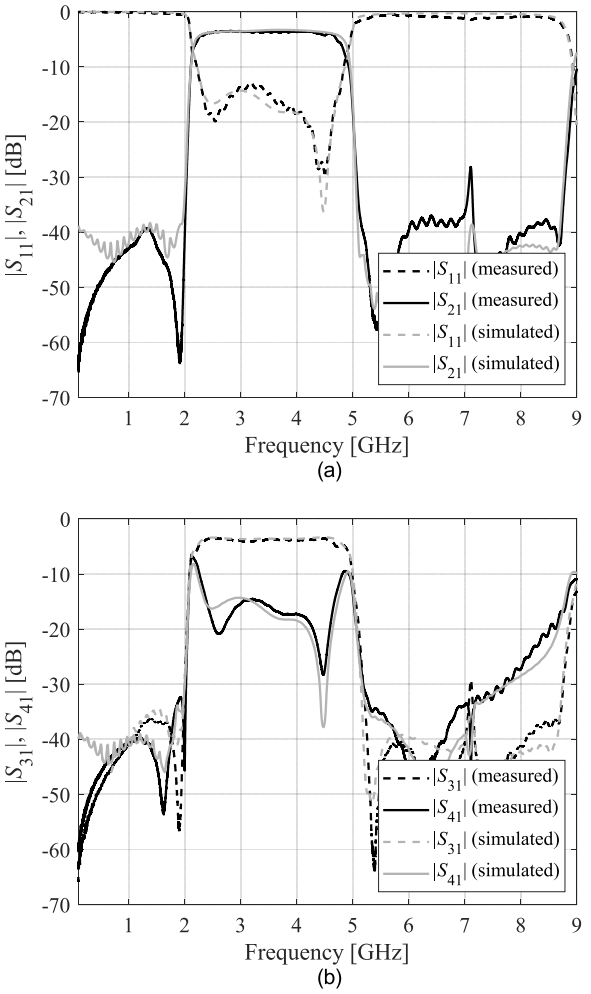

FIGURE 7. EM-simulated and measured performance of the proposed FBLC: (a) $|S_{11}|$ and $|S_{21}|$, (b) $|S_{31}|$ and $|S_{41}|$.

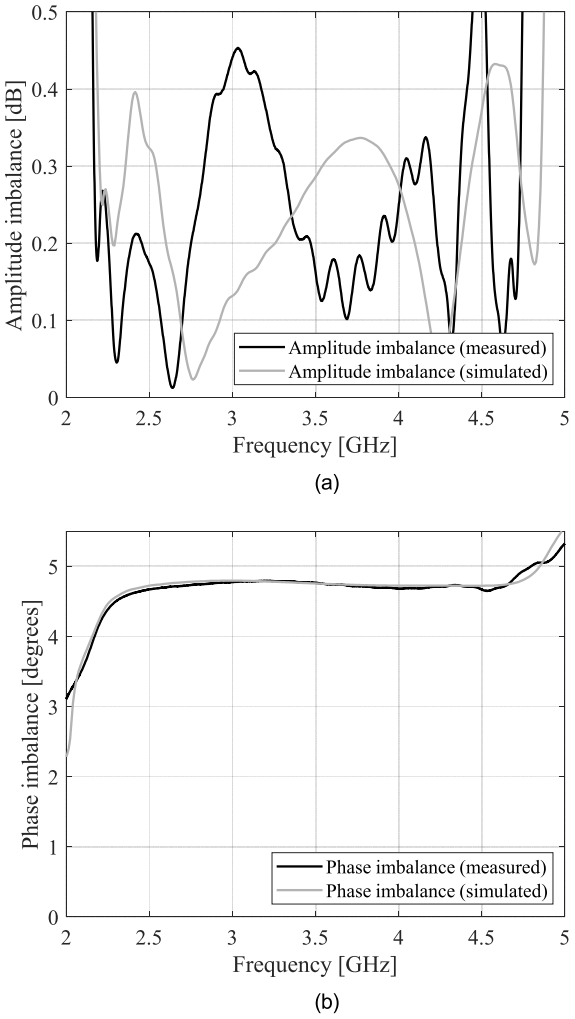

FIGURE 8. EM-simulated and measured performance of the proposed FBLC: (a) amplitude imbalance and (b) phase difference.

Here $\Delta_T = B_T C_T - A_T D_T$. In order to study the bandpass response, the S-parameters of the ATLU are determined as:

$$S_{11} = \frac{Y_0^2 - Y_{11}^2 + Y_{21}^2}{(Y_0 + Y_{11})^2 - Y_{21}^2} \tag{9}$$

$$S_{21} = \frac{-2Y_{21}Y_0}{(Y_0 + Y_{11})^2 - Y_{21}^2} \tag{10}$$

Here $Y_0 = 1/Z_0$ and $Z_0 = 50\ \Omega$. The theoretical S-parameters are obtained using equations (9) and (10) and are shown in Fig. 2(a) shows the theoretical bandpass characteristic of the proposed ATLU. Also, the proposed ATLU is analyzed using the Keysight ADS circuit simulator. Figure 2(b) shows the desired bandpass filtering response of the circuit. From the figure, it is found that the agreement between analytical and circuit simulator responses is excellent. The reflection coefficient is better than -30 dB at 3.5 GHz with wide stopband response. It can be observed that four transmission zeros are located in the frequency range from 0 to $2f_0$ at 0, 1.75, 5.25, and 7.0 GHz. This provides us with the benefit of achieving wideband highly-selective filtering BLC. Furthermore, the variation of the 3-dB fractional bandwidth (FBW) with respect to the characteristic impedance of the open-ended stub has been studied as shown in Fig. 3. It is observed that the 3-dB FBW is increased by increasing the parameter Z_{os}.

The matching property of the proposed filtering BLC is analyzed. Let us consider the relationship of characteristic impedances of the single section BLC is $Z_b = \sqrt{2}Z_a$ and θ_0 be the electrical length. Considering the input impedance at each port of the single-section BLC is matched to the ATLU, the equivalent input impedance can be expressed as:

$$Z_{eq1} = \frac{1}{1/\sin\theta_0 - j(1+\sqrt{2})\cot\theta_0} \tag{11}$$

In order to calculate the input impedance of the ATLU, the ABCD matrix is converted into Z-parameters using the

TABLE 1. The state-of-the-art wideband filtering branch-line coupler.

Refs.	f_0 (GHz)	$\|S_{11}\|/\|S_{41}\|$ (dB)	BW (%) ($\|S_{11}\|\leq 15$)	Size ($\lambda \times \lambda$)	TZs (0-2f_0)	SF (%)	OBR (dB) with frequency window (GHz)	FR	Applied techniques
[1]	1	>20	≈50	0.17 × 0.30	3	NR	>30 (1.91-4.53)	Yes	L-section and open stub
[2]	3	>16.3	50.9	0.25 × 0.75	NR	NR	NR	No	Microstrip line
[11]	2	>20	56	0.302 × 0.386	NR	NR	NR	No	Microstrip line and open stub
[12]	2	>15	>50	0.15 × 0.381	NR	NR	NR	No	Fractal geometry
[13]	2.15	>20	47	0.264 × 0.785	NR	NR	NR	No	Defected ground structure
[14]	1.1	>15	>50	0.228×0.292	NR	NR	NR	No	Unequal-length stubs
[15]	5.95	>12	65	0.25 × 0.75	NR	NR	NR	No	Microstrip-line
[17]	1.5	>15	67	0.25 × 0.75	NR	NR	NR	No	Microstrip-line
[19]	6	>20	>49	0.25 × 0.75	NR	NR	NR	No	Coupled-line and square loop
[20]	2.4	>20	50	0.245×0.665	NR	<30	>30 (0-1.48) & >20 (3.79-7.43)	Yes	Coupled-lines
[22]#	1.55	>11	110	0.92×0.76	NR	NR	>20 (2.5-30)	yes	Phase inverter & Double-sided parallel-strip line
[24]	10	>20	43.1	0.26×0.766	NR	NR	NR	No	Short/open-circuited coupled-lines
[25]	28	>20	>40	0.25×0.75	NR	NR	NR	No	Coupled-lines
[26]	1.0	>20	>15.9	0.155×0.128	2	NR	>12 (2.3-12)	No	Non-periodic stepped-impedance shunt-stub
[27]	0.9	>15	>60	0.04	NR	NR	NR	No	Shunt-open stub and meandering lines
[28]	2.45	>12	2.5	0.254×0.254	1	35	>15 (1.5-2.1 & 2.8-3.5)	Yes	Half-wave resonators
[29]	2.4	>15	3.17	0.185×0.106	2	42	>20 (1-1.8 & 3.35-8.35)	Yes	Source-load coupling
[30]	0.559	>17	≈4	0.1 × 0.1	NR	33	>20(0-0.4 & 0.9-2.6)	Yes	Equivalent K-inverters
This work	**3.5**	**>15**	**>71**	**0.25 × 0.75**	**4**	**80**	**>30 (0-1.95) & >20 (5.08-8.51)**	**Yes**	**Coupled-line, open stub and microstrip-line**

OBR: Out-of-band rejection, BW: Fractional bandwidth, TZ: Transmission zero, FR: Filtering response, NR: Not reported, #: 180° hybrid coupler.

following relationship:

$$\begin{bmatrix} Z_{11} & Z_{12} \\ Z_{21} & Z_{22} \end{bmatrix} = \begin{bmatrix} \frac{A_T}{C_T} & \frac{A_T D_T - B_T C_T}{C_T} \\ \frac{1}{C_T} & \frac{D_T}{C_T} \end{bmatrix} \tag{12}$$

The input impedance of the ATLU is defined by following [31]:

$$Z_{eq2} = \frac{Z_{22} + Z_{11}Z_{22} - Z_{12}Z_{21}}{1 + Z_{11}} \tag{13}$$

In order to match single-section BLC with the ATLU, the input impedance Z_{eq2} should be equal to Z_{eq1}. At $\theta_0 = \pi/2$, $Z_{eq1} = 1 = Z_{eq2}$. Solving equations (11), (12) and (13) using MATLAB, the circuit parameters of the filtering BLC are obtained as $Z_a = 45\ \Omega$, $Z_b = 64\ \Omega$, $Z_{0e} = 180\ \Omega$, $Z_{0o} = 80\ \Omega$, and $Z_{os} = 119\ \Omega$. Figure 4 shows the ADS-simulated S-parameter response of the FBLC. This coupler operates at 3.5 GHz with a fractional bandwidth of 72%. The return loss and isolation are greater than 15 dB in the frequency window from 2.24 GHz to 4.76 GHz. The insertion losses ($|S_{21}|$ and $|S_{31}|$) are less than 0 ± 0.5 dB for the frequency band from 2.24 to 4.76 GHz. As highlighted in Fig. 4, the out-of-band rejection is observed from 0 to 1.85 GHz and from 5.15 to 8.85 GHz considering the stopband level of 40 dB. Additionally, four transmission zeros are traced at 0, 1.75, 5.25, and 7.0 GHz. Furthermore, the selectivity is found to be better than 80% due to the presence of the transmission zeros in the passband vicinity (i.e., at 1.75 GHz and 5.25 GHz).

The power ratio of the proposed filtering branch-line coupler is k = 1 (equal power split). However, the proposed filtering coupler can be designed to provide an unequal power split. Let us consider k = 4, the design parameters of the proposed filtering coupler are calculated by following the equations (11), (12), and (13) as: $Z_a = 45\ \Omega$, $Z_b = 64\ \Omega$, $Z_{0e} = 180\ \Omega$, $Z_{0o} = 80\ \Omega$, and $Z_{os} = 119\ \Omega$. Based on these parameters, the proposed filtering coupler is simulated and shown in Fig. 5. From the figure, it is observed that the proposed coupler is capable of achieving a loose coupling power split.

III. FABRICATION, RESULTS AND DISCUSSION

To validate the proposed circuit architecture, a prototype of wideband filtering BLC centered at 3.5 GHz is designed and fabricated on Rogers AD250 substrate ($\varepsilon_r = 2.5$, H = 0.762 mm). The proposed bandpass filtering branch-line coupler operating at 3.5 GHz is suitable for WiMAX and 5G applications but not limited to. However, the proposed filtering BLC can be used for WiFi (5GHz), Bluetooth (2.4), and WLAN (2.4 GHz, 3.6 GHz, 4.9 GHz, 5 GHz, and 5.9 GHz bands) applications by re-calculating the physical dimensions at the corresponding frequency of operation. The final layout of the FBLC with optimized dimensions is shown in Fig. 6(a), whereas Fig. 6(b) shows the fabricated FBLC.

The scattering parameters are measured using a two-port HP vector network analyzer and compared to the EM simulated results, as shown in Fig. 7. The magnitude responses ($|S_{k1}|$, k = 1, 2, 3, 4) are illustrated in Fig. 7(a) and 7(b). The measurement results demonstrate that the fabricated circuit prototype offers a high-selectivity wideband bandpass filtering characteristic. It also exhibits a fractional bandwidth of over 71%, considering the return loss ($|S_{11}|$) and isolation ($|S_{41}|$) greater than 15 dB. At the center frequency of 3.5 GHz, the values of $|S_{11}|$, $|S_{21}|$, $|S_{31}|$, and $|S_{41}|$ are 15.5, 2.98, 3.01, 15.4 dB, respectively. The amplitude imbalance ($|S_{21}| - |S_{31}|$) and the phase difference between the two output ports have been shown in Fig. 8. The prototype achieves a low amplitude imbalance of 0.5 dB, and a phase difference of 90°± 5° over the frequency range of 2.25 GHz to 4.74 GHz.

The selectivity factor of the bandpass filtering response is computed by following the equation [33]:

$$S.F.(\%) = \frac{\Delta f_{3dB}}{\Delta f_{30dB}} \times 100 \tag{14}$$

Here, $\Delta f_{3\text{dB}}$ and $\Delta f_{30\text{dB}}$ are defined as 3-dB bandwidth and 30-dB bandwidth, respectively. From the table, it is observed that the proposed filtering BLC achieves the highest selectivity when compared with existing works in [1]–[30].

The proposed filtering BLC exhibits superior performance when compared to the state-of-the-art circuits [1], [2], [11]–[15], [17], [19], [20], [22], and [24]–[30] as indicated in Table 1. In particular, our FBLC achieves the highest bandwidth with a larger number of transmission zeros, along with wide stopband characteristics except [22]. Although the sizes of the BLCs reported in [1], [11], [12], [14], and [26], [27] are smaller than that of the proposed FBLC, the mentioned designs feature limited bandwidth and unwanted harmonics while providing no filtering capability. The proposed filtering coupler achieves 40-percent broader bandwidth and is highly selective when compared to [20]. Compared to [22], the proposed coupler provides greater features in terms of return loss/isolation, high-selectivity, transmission zeros, and compact size (73-percent smaller than [22]) except fractional bandwidth. The proposed coupler provides higher bandwidth, high-selectivity, filtering response, and good out-of-band rejection when compared to [24]–[27]. The works [28]–[30] report compact BLCs with filtering responses, yet these designs suffer from very narrow bandwidth (<4%), and inferior stopband level (<20 dB). As a comparison, the bandwidth of the coupler proposed in this letter is approximately 17 times broader. The aforementioned data justifies a conclusion that the proposed FBLC is an attractive alternative over the state-of-the-art circuits of the considered class.

IV. CONCLUSION

This paper presented a novel design of filtering BLC featuring high selectivity and wideband characteristics. In our design, each port of the traditional single-section BLC is supplemented by an ATLU consisting of a coupled-line and an open-ended stub, which allows for achieving a broadband and filtering response. The analysis of the working principle and a description of the design procedure of the FBLC has been followed by experimental validation of the prototype circuit developed to operate at 3.5 GHz. The FBLC offers over 71% fractional bandwidth for return/isolation loss better than 15 dB, an amplitude imbalance of 0.5 dB, as well as selectivity better than 80% with the stopband level greater than 30 dB. Comprehensive benchmarking demonstrates the superior performance of the proposed design over the state-of-the-art circuits.

REFERENCES

[1] H. Ahn and M. M. Tentzeris, "Arbitrary power-division branch-line hybrids for high-performance, wideband, and selective harmonic suppressions from 2f0," *IEEE Trans. Microw. Theory Techn.*, vol. 67, no. 3, pp. 978–987, Mar. 2019.

[2] S. Lee and Y. Lee, "Wideband branch-line couplers with single-section quarter-wave transformers for arbitrary coupling levels," *IEEE Microw. Wireless Compon. Lett.*, vol. 22, no. 1, pp. 19–21, Jan. 2012.

[3] R. K. Barik, K. V. Phani Kumar, and S. S. Karthikeyan, "A compact wideband harmonic suppressed 10 dB branch line coupler using cascaded symmetric PI sections," *Microw. Opt. Technol. Lett.*, vol. 58, no. 7, pp. 1610–1613, Jul. 2016.

[4] Q. Wu, Y. Yang, M. Lin, and X. Shi, "Miniaturized broadband branch-line coupler," *Microw. Opt. Technol. Lett.*, vol. 56, no. 3, pp. 740–743, Mar. 2014.

[5] H.-J. Yoon and B.-W. Min, "Two section wideband 90° hybrid coupler using parallel-coupled three-line," *IEEE Microw. Wireless Compon. Lett.*, vol. 27, no. 6, pp. 548–550, Jun. 2017.

[6] Z. Qamar, W. S. Chan, and H. Derek, "Wide bandwidth arbitrary phase difference branch line coupler," *Microw. Opt. Technol. Lett.*, vol. 59, no. 9, pp. 2241–2245, Jun. 2017.

[7] Z. Qamar, S. Y. Zheng, W. S. Chan, and D. Ho, "Coupling coefficient reconfigurable wideband branch-line coupler topology with harmonic suppression," *IEEE Trans. Microw. Theory Techn.*, vol. 66, no. 4, pp. 1912–1920, Apr. 2018.

[8] P. Kurgan and S. Koziel, "Rapid surrogate-assisted design optimization of minimum-size broadband branch-line couplers with variable topology," *Int. J. RF Microw. Comput.-Aided Eng.*, vol. 28, no. 5, Jun. 2018, Art. no. e21255.

[9] L. Chiu and Q. Xue, "Investigation of a wideband 90° hybrid coupler with an arbitrary coupling level," *IEEE Trans. Microw. Theory Techn.*, vol. 58, no. 4, pp. 1022–1029, Apr. 2010.

[10] Q. Wu, Y. Yang, Y. Wang, X. Shi, and M. Yu, "Characteristic impedance control for branch-line coupler design," *IEEE Microw. Wireless Compon. Lett.*, vol. 28, no. 2, pp. 123–125, Feb. 2018.

[11] Y.-H. Chun and J.-S. Hong, "Compact wide-band branch-line hybrids," *IEEE Trans. Microw. Theory Techn.*, vol. 54, no. 2, pp. 704–709, Feb. 2006.

[12] W.-L. Chen, G.-M. Wang, and C.-X. Zhang, "Miniaturization of wideband branch-line couplers using fractal-shaped geometry," *Microw. Opt. Technol. Lett.*, vol. 51, no. 1, pp. 26–29, Jan. 2009.

[13] P. Kurgan and M. Kitlinski, "Novel doubly perforated broadband microstrip branch-line couplers," *Microw. Opt. Technol. Lett.*, vol. 51, no. 9, pp. 2149–2152, Sep. 2009.
[14] V. K. Velidi, B. Patel, and S. Sanya, "Harmonic suppressed compact wideband branch-line coupler using unequal length open-stub units," *Int. J. RF Microw. Comput.-Aided Eng.*, vol. 21, no. 1, pp. 115–119, Jan. 2011.
[15] H. Rashid, P. Y. Aghdam, D. Meledin, V. Desmaris, and V. Belitsky, "Wideband planar hybrid with ultralow amplitude imbalance," *IEEE Microw. Wireless Compon. Lett.*, vol. 27, no. 3, pp. 230–232, Mar. 2017.
[16] R. K. Barik, R. Rajender, and S. S. Karthikeyan, "A miniaturized wideband three-section branch-line hybrid with harmonic suppression using coupled line and open-ended stubs," *IEEE Microw. Wireless Compon. Lett.*, vol. 27, no. 12, pp. 1059–1061, Dec. 2017.
[17] A. Buesa-Zubiria and J. Esteban, "Design of broadband doubly asymmetrical branch-line directional couplers," *IEEE Trans. Microw. Theory Techn.*, vol. 68, no. 4, pp. 1439–1451, Apr. 2020.
[18] R. K. Barik, Q. S. Cheng, N. C. Pradhan, and K. S. Subramanian, "Highly miniaturized wideband 3-dB branch-line hybrid with second harmonic-suppression," *Microw. Opt. Technol. Lett.*, vol. 62, no. 6, pp. 2248–2256, Jun. 2020.
[19] W. A. Arriola, J. Y. Lee, and I. S. Kim, "Wideband 3 dB branch line coupler based on λ/4 open circuited coupled lines," *IEEE Microw. Wireless Compon. Lett.*, vol. 21, no. 9, pp. 486–488, Sep. 2011.
[20] W. Nie, K.-D. Xu, M. Zhou, L.-B. Xie, and X.-L. Yang, "Compact narrow/wide band branch-line couplers with improved upper-stopband," *AEU-Int. J. Electron. Commun.*, vol. 98, pp. 45–50, Jan. 2019.
[21] K.-D. Xu, D. Li, and Y. Liu, "High-selectivity wideband bandpass filter using simple coupled lines with multiple transmission poles and zeros," *IEEE Microw. Wireless Compon. Lett.*, vol. 29, no. 2, pp. 107–109, Feb. 2019.
[22] Q.-S. Shen, M.-J. Gao, L.-S. Wu, and X.-L. Zhou, "Ultra-wideband filtering 180° hybrid coupler with super wide upper stopband using swap phase inverter and electromagnetic bandgap structures on double-sided parallel-strip line," *IEEE Access*, vol. 6, pp. 41099–41106, 2018.
[23] H. Zhu and Y. J. Guo, "Wideband filtering phase shifter using transversal signal-interference techniques," *IEEE Microw. Wireless Compon. Lett.*, vol. 29, no. 4, pp. 252–254, Apr. 2019.
[24] Y. Haoka, T. Kawai, and A. Enokihara, "X-band broadband branch-line coupler with loose coupling utilizing short-/open-circuited coupled-transmission lines," in *Proc. Asia–Pacific Microw. Conf. (APMC)*, Nov. 2018, pp. 1498–1500.
[25] Y. Haoka, T. Kawai, and A. Enokihara, "Design of broadband branch-line couplers utilizing coupled transmission lines at Ka-band," in *Proc. 12th Global Symp. Millim. Waves (GSMM)*, May 2019, pp. 41–43.
[26] J. Coromina, P. Velez, J. Bonache, and F. Martin, "Branch line couplers with small size and harmonic suppression based on non-periodic step impedance shunt stub (SISS) loaded lines," *IEEE Access*, vol. 8, pp. 67310–67320, 2020.
[27] K. V. P. Kumar and A. J. Alazemi, "A flexible miniaturized wideband branch-line coupler using shunt open-stubs and meandering technique," *IEEE Access*, vol. 9, pp. 158241–158246, 2021.
[28] T. Lin, C. Lin, K. Huang, and J. Kuo, "Compact branch-line coupler filter with transmission zeros," in *Proc. Asia–Pacific Microw. Conf. (APMC)*, 2015, pp. 1–3.
[29] T. Lin, J. Wu, and J. Kuo, "Compact filtering branch-line coupler with source-load coupling," in *Proc. Int. Workshop Electromagn., Appl. Student Innov. Competition (iWEM)*, 2016, pp. 1–3.
[30] R. N. Du, Z. B. Weng, and C. Zhang, "A miniaturized filtering 3-dB branch-line hybrid coupler with wide suppression band," *Prog. Electromag. Res. Lett.*, vol. 73, pp. 83–89, 2018.
[31] T. Jensen, V. Zhurbenko, V. Krozer, and P. Meincke, "Coupled transmission lines as impedance transformer," *IEEE Trans. Microw. Theory Techn.*, vol. 55, no. 12, pp. 2957–2965, Dec. 2007.
[32] D. M. Pozar, *Microwave Engineering*. New York, NY, USA: Wiley, 2005.
[33] J. S. Hong and M. J. Lancaster, *Microstrip Filters for RF/Microwave Applications*. New York, NY, USA: Wiley, 2001.

RUSAN KUMAR BARIK (Member, IEEE) received the B.Tech. degree in electronics and communication engineering from the Biju Patnaik University of Technology, Rourkela, India, in 2012, and the M.Tech. degree in communication systems design and the Ph.D. degree in electronics engineering from the Indian Institute of Information Technology, India, in 2015 and 2018, respectively. He joined the Department of Electronics and Communication Engineering, Christ University, Bengaluru, India, as an Assistant Professor, in 2018. In 2019, he joined as a Postdoctoral Researcher at the Department of Electrical and Electronic Engineering, Southern University of Science and Technology, Shenzhen, China. Currently, he is working as a Postdoctoral Researcher with the Engineering Optimization and Modeling Center (EOMC), Department of Electrical Engineering, Reykjavik University, Iceland. His research interests include multiband microwave devices, SIW components, surrogate-based modeling, and optimization.

SLAWOMIR KOZIEL (Fellow, IEEE) received the M.Sc. and Ph.D. degrees in electronic engineering from the Gdańsk University of Technology, Poland, in 1995 and 2000, respectively, and the M.Sc. degree in theoretical physics, the M.Sc. degree in mathematics, and the Ph.D. degree in mathematics from the University of Gdańsk, Poland, in 2000, 2002, and 2003, respectively. He is currently a Professor with the Department of Engineering, Reykjavik University, Iceland. His research interests include CAD and modeling of microwave and antenna structures, simulation-driven design, surrogate-based optimization, space mapping, circuit theory, analog signal processing, and evolutionary computation and numerical analysis.

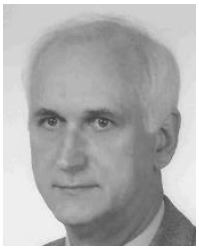

STANISLAW SZCZEPANSKI received the M.Sc. and Ph.D. degrees in electronic engineering from the Gdańsk University of Technology, Poland, in 1975 and 1986, respectively. In 1986, he was a Visiting Research Associate with the National Polytechnic Institute of Toulouse (INPT), Toulouse, France. From 1990 to 1991, he was with the Department of Electrical Engineering, Portland State University, Portland, OR, USA, on a Kosciuszko Foundation Fellowship. From August 1997 to September 1998, he was a Visiting Professor with the Faculty of Engineering and Information Sciences, University of Hertfordshire, Hatfield, U.K. He is currently a Professor with the Department of Microelectronic Systems, Faculty of Electronics, Telecommunications and Informatics, Gdańsk University of Technology. He has published more than 160 papers and holds three patents. His teaching and research interests include circuit theory, fully integrated analog filters, high-frequency transconductance amplifiers, analog integrated circuit design, and analog signal processing.